

## ARTICLE

# The robustness of reinforced concrete tied arch bridges: A case study

Antonio Formisano<sup>1</sup>  | Matteo Felitti<sup>2</sup> | Francesco Oliveto<sup>3</sup> | Lorenzo Mendicino<sup>4</sup>

<sup>1</sup>Department of Structures for Engineering and Architecture, University of Naples Federico II, Naples, Italy

<sup>2</sup>Engineering & Concrete Consulting, Vietri di Potenza (PZ), Italy

<sup>3</sup>Freelance Engineer, Viggianello (PZ), Italy

<sup>4</sup>Stacec SRL Company, Bovalino (RC), Italy

## Correspondence

Antonio Formisano, Department of Structures for Engineering and Architecture, University of Naples Federico II, Naples, Italy.  
Email: [antoform@unina.it](mailto:antoform@unina.it)

## Abstract

The robustness of a structural systems is understood as their ability to prevent or reduce the consequences of a local (exceptional and/or extreme) event. The current work aims to address the issues related to the evaluation of robustness of structures with incorporated damage. The case study of an existing reinforced concrete arch bridge is investigated in terms of robustness considering the variation of both the cracking state from concrete spalling and the corrosion of reinforcement bars. The damage variation related to these different matters is assessed both in terms of intensity and occurrence in the various structural elements of the bridge. Finally, the structural robustness index is estimated through push-down analysis to make an overall assessment of the bridge behavior.

## KEYWORDS

arch bridge, corrosion, push-down analysis, reinforced concrete, robustness

## 1 | INTRODUCTION

The durability problems of reinforced concrete structures, which are deeply felt by researchers and designers, are often related to corrosion degradation. Typically, these harmful phenomena for the structural health are induced by carbonation or attack of substances containing chlorides.

In fact, over time, reinforced concrete can be subjected to various attack type:

- by carbonation, which consists in the neutralization of the concrete alkalinity by carbon dioxide from the external environment, with destruction of the oxide film used to protect the bars;

- by penetration of chlorides, when a certain noise content is reached and exceeded on the surface of the reinforcements, so to destroy the protective film;
- by dispersed currents, which interfere with the reinforcement bars, passing in some parts from concrete to bars and in other zones from bars to concrete.

When the passivity conditions cease to exist, the corrosive process of the reinforcement bars, which is of an electrochemical nature, can take place if the concrete meets water and oxygen. The ignition and propagation phases involve the following sub-phases (Figure 1a,b):

- Initial phase without corrosion (depasivation) for  $t = t_{(1)}$ . It persists until the concentration of aggressive

This is an open access article under the terms of the [Creative Commons Attribution-NonCommercial-NoDerivs](https://creativecommons.org/licenses/by-nc-nd/4.0/) License, which permits use and distribution in any medium, provided the original work is properly cited, the use is non-commercial and no modifications or adaptations are made.

© 2023 The Authors. *Structural Concrete* published by John Wiley & Sons Ltd on behalf of International Federation for Structural Concrete.

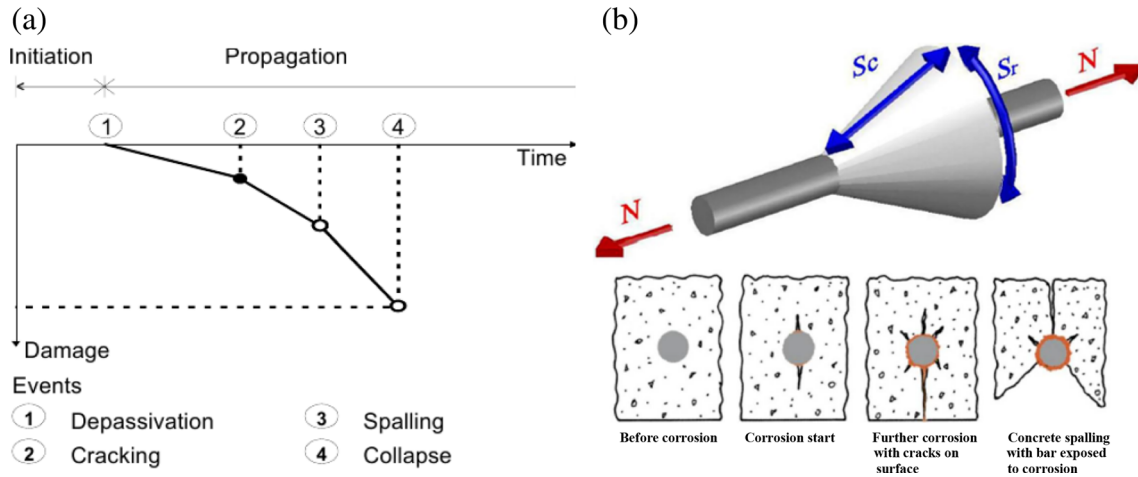
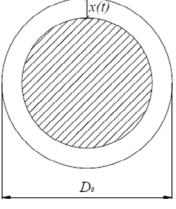
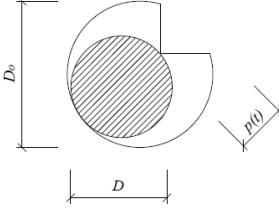
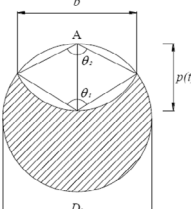


FIGURE 1 (a) Schematic representation of degradation as a function of damage; (b) cover ejection, splitting and spalling failure.<sup>1</sup>

TABLE 1 Degradation models for decrease of the bar resistant cross-section.

Uniform corrosion	Localized corrosion by Rodriguez et al. <sup>2</sup>	Localized corrosion by Val et al. <sup>3</sup>
		
$\delta = \frac{x}{D_0} \rightarrow$ $A_s(\delta) = A_{s0} \cdot [1 - \delta_{As,u}(\delta)]$ $\delta_{As,u}(\delta) = 1$ if $\delta > 0.5$ $\delta_{As,u}(\delta) = 4 \cdot \delta \cdot (1 - \delta)$ if $0 \leq \delta \leq 0.5$	$\delta \cdot R$ $A_s(\delta R) = A_{s0} \cdot [1 - \delta_{As,pR}(\delta R)]$ $\delta_{As,pR}(\delta R) = \begin{cases} 2\delta R - (\delta R)^2 & \text{if } 0 \leq \delta R \leq 1 \\ 1 & \text{if } \delta R \leq 1 \end{cases}$	$\begin{cases} A_{pit}(t) = A_1 + A_2 & \text{if } p(t) \leq \frac{D_0}{\sqrt{2}} \\ A_{pit}(t) = A_0 - A_1 + A_2 & \text{if } \frac{D_0}{\sqrt{2}} \leq p(t) \leq D_0 \\ A_{pit}(t) = A_0 & \text{if } p(t) \geq D_0 \end{cases}$ $\alpha_{pit} = A_{pit}(t)/A_0$

agents does not exceed certain limits for the lack of passivation of reinforcing steel;

- First propagation phase (cracking) up to  $t = t_{(2)} = t_{cr1}$ , where the first crack occurs in the concrete surface due to the reinforcement corrosion;
- Second propagation phase (spalling), with a higher propagation speed due to the presence of cracks, up to  $t = t_{(3)} = t_{cr2}$ , when the operation limit state is no longer satisfied with the concrete spalling;
- Last propagation phase (collapse), denoted by  $t = t_{(4)} = t_u$ , when the resistance reduction is such that the demands imposed by the ultimate limit state are no longer met.

The aim of the present work is the automatic implementation of corrosion degradation models of bridges through a non-linear fiber FEM model, having a force-based formulation in the field of large displacements

which is setup in the FATANEXT NL calculation code produced by the STACEC Srl company. The implemented methodology is applied to a tied arch type concrete arch bridge dating back to 1930. With this approach, different corrosion degradation scenarios related to any space-time distributions with a reasonably reduced time are examined. Therefore, as final goal of the study, the robustness indicators for different scenarios and degrees of corrosion are assessed, so leading to the evaluation of either the capacity or the residual life of the structure.

## 2 | MODELING OF CORROSION DEGRADATION MECHANISMS

The corrosion phenomenon has a considerable influence on the mechanical behavior of reinforced concrete structural elements with reference to:

- Reduction of the cross-section of reinforcing bars;
- Decrease of the mechanical features (strength and ductility) of steel;
- Cracking of concrete with reduced compressive strength;
- Deterioration of the adhesion mechanism.

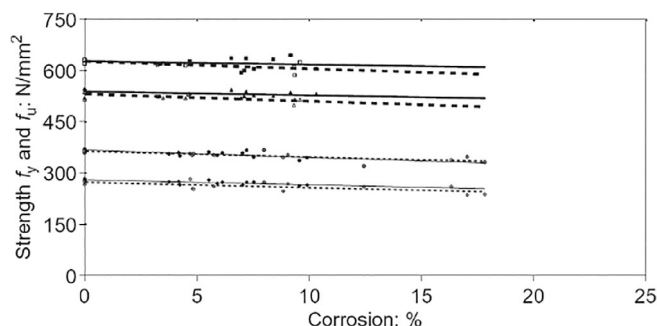


FIGURE 2 Residual resistance of corroded reinforcing bars.<sup>6,7</sup>

Corrosion leads to the reduction of both the bar cross-section and the elongation capacity of the intact part of the reinforcement bar, with all the negative consequences on structural ductility. Iron oxide (rust), which is the product of the corrosion process, generates a volume larger than that of the basic metal. This produces radial compression stresses ( $S_c$ ) in the concrete surrounding the bar and, for equilibrium, the emergence of circumferential tensile stresses ( $S_r$ ). When these latter pressures reach the concrete tensile strength, the formation of cracks orthogonal to the tensile isostatics occur, usually leading toward the complete expulsion of the cover (spalling failure of Figure 1b).

The concrete-bars perfect bond is one of the fundamental properties ruling the satisfactory behavior of reinforced concrete elements. It is worth noticing that the adherence between materials is also influenced by corrosion through the following mechanisms:

FIGURE 3 Concrete parts damaged by corrosion of bars.<sup>7</sup>

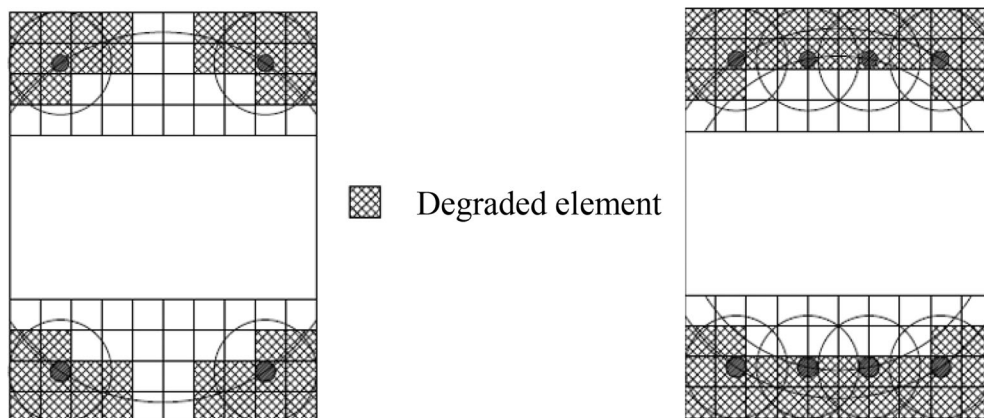


FIGURE 4 Picture and front view of the bridge on the Cassibile river.

- cracking of concrete;
- change of properties at the steel-to-concrete interface;
- less confinement of concrete due to the corrosion of stirrups;
- instability of longitudinal reinforcement due to concrete spalling;
- reduction of the cyclic response under horizontal actions with decrease of both the dissipated energy and the rotational capacity of structural elements.

The reduction of the reinforcement bar cross-section can be evaluated according to the degradation models depicted in Table 1.

The variation of the steel mechanical properties according to the Val et al.'s model<sup>3</sup> can be determined based on the following linear relationship (Figure 2):

$$f = (1 - \beta \cdot Q_{\text{corr}}) \cdot f_0 \quad (1)$$

where  $f_0$  is the yielding or ultimate strength of the intact bar,  $Q_{\text{corr}}$  is the corrosion level [%] and  $\beta$  is equal

to 0.5.  $Q_{\text{corr}}$  is calculated by means of the Stewart's formulation<sup>4</sup>:

$$Q_{\text{corr}} = \alpha_{\text{pit}} = A_{\text{pit}}(t)/A_0 \quad (2)$$

where  $A_{\text{pit}}$  is the corroded bar area, function of the time  $t$ , and  $A_0$  is the original area of the element without corrosion.

In the case of localized corrosion with the Rodriguez's approach,<sup>2</sup> uniform corrosion formulas can be used considering the pitting factor  $R$ . For the pit model following the Val et al.'s approach,<sup>3</sup> the reduction of the steel ultimate deformation from the value  $\epsilon'_{\text{su}} = \epsilon_{\text{su}}$ , for virgin material, up to  $\epsilon'_{\text{su}} = \epsilon_{\text{sy}}$ , for the complete ductility loss, is evaluated through the following formula [8]:

$$\epsilon'_{\text{su}} = \epsilon_{\text{sy}} + (\epsilon_{\text{su}} - \epsilon_{\text{sy}}) \cdot \left(1 - \frac{\alpha_{\text{pit}}}{\alpha_{\text{pit,max}}}\right) \text{ if } \alpha_{\text{pit}} \leq \alpha_{\text{pit,max}} \quad (3)$$

The trend is linear and is proportional to the reduction of area caused by pitting, as defined in the following expression:

TABLE 2 Geometrical features and reinforcement type of bridge sections.

Bridge geometry									
$L$ [m]	$m$ [m]	$p$ [m]	$w$ [m]	$f$ [m]	$L/m$ [m]				
30.00	6.00	8.30	7.50	5.00	$\leq 1/5$ —eliminated thrust bridge				
Geometry of sections									
Lateral main beams		Central main beam		Secondary beams		Tie-beams $b \times h$ [cm]	Arches		Slab $h$ [cm]
$b$ [cm]	$h$ [cm]	$b$ [cm]	$h$ [cm]	$b$ [cm]	$h$ [cm]		$b$ [cm]	$h$ [cm]	
50	80	20	80	25	80	$36 \times 30$	50	100	12–15
Materials—Knowledge level LC2 $\rightarrow$ FC = 1.20									
Calcestruzzo						Acciaio			
$f_{\text{cm}}$ [Mpa]	$f_{\text{cm-res}}$ [%]		$\epsilon_{\text{cu}}$ [%]	$\epsilon_{\text{tu}}$ [%]	$f_{\text{ym}}$ [Mpa]	$\epsilon_{\text{cu}}$ [%]		$\epsilon_{\text{tu}}$ [%]	
18.00	20		0.20	0.35	320.0	6.00		10.00	
Reinforcement of cross-sections									
Section type	Longitudinal bars			Stirrups					
	Down	Top	Intermediate	Left support	Middle	Right support			
Lateral main beams	5 $\phi$ 20	5 $\phi$ 20	1 + 1 $\phi$ 20	1 $\phi$ 6/25	1 $\phi$ 6/25	1 $\phi$ 6/25			
Central main beam	3 $\phi$ 20	3 $\phi$ 20	2 + 2 $\phi$ 20	1 $\phi$ 6/20	1 $\phi$ 6/20	1 $\phi$ 6/20			
Secondary beams	3 $\phi$ 18	3 $\phi$ 18	-	1 $\phi$ 6/20	1 $\phi$ 6/20	1 $\phi$ 6/20			
Tie-beams	5 $\phi$ 20	5 $\phi$ 20	1 $\phi$ 20	1 $\phi$ 8/15	1 $\phi$ 8/15	1 $\phi$ 8/15			
Arches	6 $\phi$ 20	6 $\phi$ 20	2 + 2 $\phi$ 20	1 $\phi$ 8/20	1 $\phi$ 8/20	1 $\phi$ 8/20			

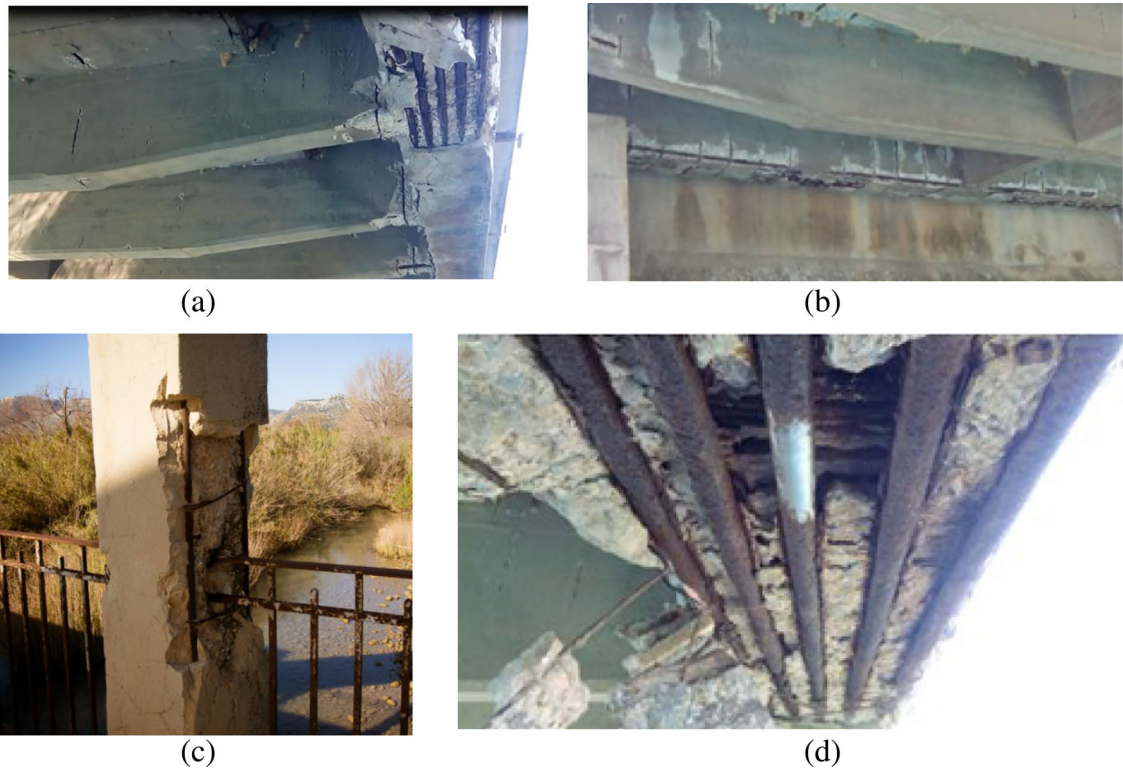


**FIGURE 5** Views of transverse beams (a), longitudinal beams (b) and tie-beams (c) with spalling of concrete cover, corrosion of the longitudinal reinforcement (d) and flaking of the transverse reinforcement.

$$\alpha_{\text{pit}} = A_{\text{pit}}(t)/A_0 \quad (4)$$

From several experimental studies conducted to evaluate the parameter  $\alpha_{\text{pit,max}}$ ,<sup>4</sup> it is seen that it oscillates between 0.5 and 0.1.

The concrete degradation is herein modeled so to grasp in a simple way the main consequences on the bridge global behavior. In particular, the damage to the material in the area surrounding the corroded reinforcing bars with a compressive strength decreases.<sup>5</sup> The concrete parts located near the reinforcing bars, which could be damaged, must therefore be identified. Unlike other simplified models,<sup>8</sup> where the characteristics of the degraded material are assigned a priori to all the elements of the compressed zone cover, the model proposed in Reference 7 foresees that only the elements included in a circle of the bar radius equal to the cover are subject to degradation; moreover, only in the elements outside the confined core the degradation is activated (Figure 3).

Despite being a simplified model, it can be used to find the different damage mechanism dependent on the arrangement of bars: if the bars are very close to each other, the cover will tend to detach according to a horizontal fracture plane; instead, if the bars are far away or

are placed in the corners, the damage will be concentrated in the part near the bar, with inclined fracture planes. Degradation of the compressive strength for cracked concrete elements is modeled with reference to the following relationship<sup>7</sup>:

$$f_{c,\text{red}} = f_c / (1 + K \cdot \varepsilon_t / \varepsilon_{c0}) \quad (5)$$

where  $K$  is a coefficient related to the roughness and diameter of the bars, which can be assumed equal to 0.1 for ribbed bars of medium diameter;  $f_c$  is the peak value of the compression strength corresponding to the strain  $\varepsilon_{c0}$ , which can be calculated as:

$$\varepsilon_{c0} = 0.0017 + 0.0010 \cdot (f_{cm}/70) \quad (6)$$

being  $f_{cm} = f_c + 8$  (MPa) the concrete average strength.  $\varepsilon_t$  represents the swelling transverse deformation of the section, which can be calculated as:

$$\varepsilon_t = n_{\text{bars}} \cdot w / b_i \quad (7)$$

where  $b_i$  is the width of the considered section part,  $w$  is the average slot opening for each bar and  $n_{\text{bars}}$  is the number of bars present in  $b_i$ .

### 3 | THE CASE STUDY

To better understand the effect of pitting corrosion degradation as a function of the corrosive state on the structural robustness of bridges, a case study is herein examined.

The SS 115 road, which connects Trapani with Syracuse passing through Agrigento, crosses the Cassibile river near the municipality with a reinforced concrete tied arch bridge with eliminated thrusts (Figure 4a,b).

This artifact was built in 1930 by the Ferrobeton enterprise. This bridge static scheme was largely used for RC constructions in the pre-war period for river crossings in flat areas, where there is a limited height difference between the roadway and the substructures.

The bridge type with eliminated thrust (tied arch type) under study is made of a deck sustained by a couple of overhanging arches through tie-beams. The bridge has a span with length ( $L$ ) of about 30.00 m, with a rise ( $m$ ) of 6.00 m and a hydraulic franc ( $f$ ) of 5.00 m; the pitch ( $p$ ) between arches is 8.30 m, while the roadway width ( $w$ ) is 7.50 m. Therefore, it has a ratio between rise and span equal to 1/5, which represents a typical average value for bridges with eliminated thrust.<sup>9</sup> The superstructure rests on rc piles. The deck consists of a 15 cm thick slab armed with smooth steel bars and is supported by a sequence of beams, which have rectangular cross-section with height of 0.85 m and base of 0.25 m and are alternatively sustained by tie-beams. These beams, having pitch of 1.40 m, have a slightly tapered section at their ends, which are connected to the edge longitudinal beams. Such latter members, fulfilling the task of thrust bearing, also have a rectangular section with a height of 0.85 m and a base equal to 0.50 m. The arches are connected transversely by two  $0.25 \times 0.80$  m beams having the bracing function of the structure. The tie-beams, 10 for each arch, are placed with an interaxis of 2.86 m and have a  $0.36 \times 0.30$  m rectangular cross-section. The road is completed with an original massif and a pavement package that, due to the succession of numerous stretches of bituminous conglomerate, has reached a thickness varying between 0.16 and 0.19 m.

Table 2 shows the main geometrical features of structural elements, the number and type of reinforcement bars and the physical-mechanical properties of the bridge materials.

The bridge over the Cassibile river had a recent temporary closure, prudently adopted following the results of a preliminary investigations campaign aimed at assessing its safety conditions. In fact, considering the significant importance of the bridge within the road system of that zone, the Managing Body decided to deepen the study to better define the bridge service capacity. In the following the real state of the structure and the related degradation conditions are

presented. From the bridge observation, it is apparent that most of the structural elements show an advanced state of degradation, which is manifested by the disintegration or detachment of the concrete cover (Figure 5). In fact, the bridge surfaces showing cover spalling with bars exposed to environmental actions are very extensive. Longitudinal reinforcing bars with diameter of 20 mm do not yet show worrying signs of section reduction, while stirrups are strongly affected by corrosion. The degradation is due to a set of causes, such as the high permeability of the concrete, the aggressive environmental conditions aging on the structure and a prolonged leaching of the bridge lateral and intradosal surfaces due to rainwater coming from the road. Much more information on the health state of the bridge are available in Reference 9.

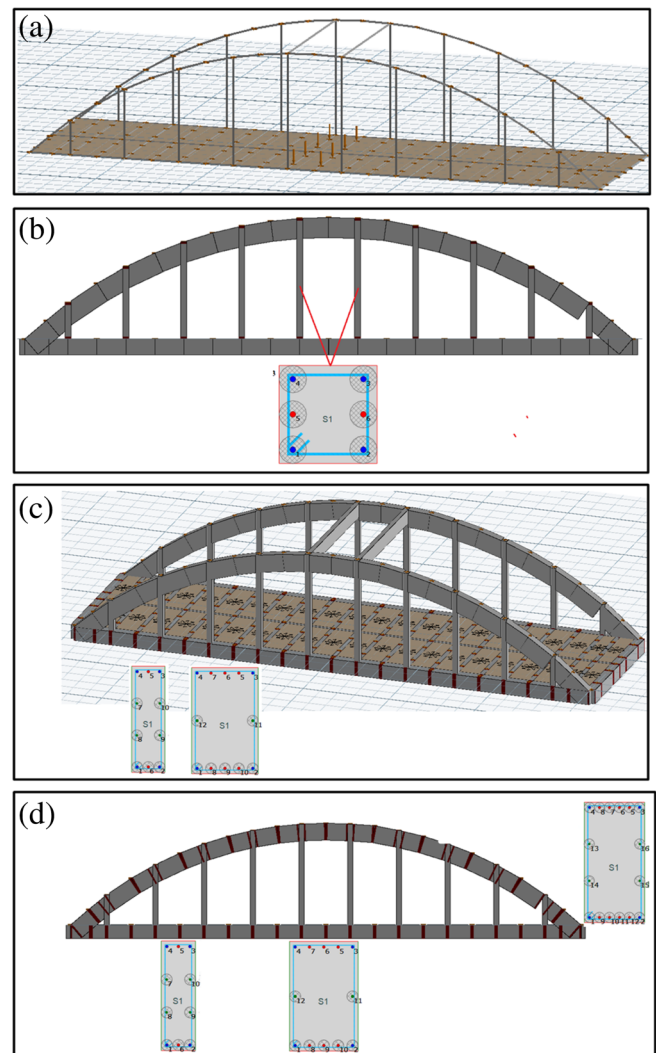


**FIGURE 6** FEM model of the bridge with loads in the middle of the deck (a) and degraded structural models: (b) deterioration scenario I with corrosion of tie-beams ( $x_{\text{corr}} = 1$  and  $R = 3$ ); (c) deterioration scenario II with corrosion of deck beams ( $x_{\text{corr}} = 1$  and  $R = 3$ ); (d) deterioration scenario III with corrosion of deck beams and lateral arches ( $x_{\text{corr}} = 1$  and  $R = 3$ ).

Signs of a cortical healing operation are detected, but they are considered as inadequate, as shown in the above photographic documentation. The reasons of this insuccess are due to the inadequacy of the mechanical characteristics of the filler material, too rigid compared to the base material and, probably, to the inadequate support preparation before the intervention.

From in situ survey, it is not possible to detect the bridge support types. Therefore, in the numerical analysis reference is made to the construction technique of the time, which provided for this type of structures external constraints with a hinge on one side and a sliding support on the other side.<sup>10</sup>

## 4 | ANALYSIS METHODOLOGY AND FEM MODELING

The robustness evaluation of the bridge, which is done through push-down analysis based on traffic loads applied to both the original model and that damaged by pitting corrosion of longitudinal reinforcements, is made through the following steps:

1. Assessment stage of the influence of the mobile loads defined as loading scheme n.1 according to the Italian standard code NTC 2018<sup>11</sup>;

2. Evaluation phase considering both different degradation scenarios and position of the mobile loads in the loading scheme n.1 as detrimental issues.

The considered degradation scenarios foresee the presence of corrosion on the following structural elements:

- Tie-beams connecting lateral arches with deck side beams;
- Longitudinal and transverse beams of the reinforced concrete deck;
- Reinforced concrete deck and lateral arches.

The corrosion of the structural elements foreseen by the hypothesized scenarios is based on both a corrosion depth  $x_{\text{corr}} = 1.00$  mm and a pitting factor  $R = 3$ .<sup>12</sup> About the distribution of corroded reinforcements of structural elements, the following hypotheses are made:

- Main longitudinal beams and connecting transverse beams: corrosion of lower longitudinal reinforcements and intermediate bars;
- Tie-beams: corrosion of all longitudinal reinforcement bars;
- Side arches: corrosion of the lower, upper and intermediate longitudinal reinforcements.

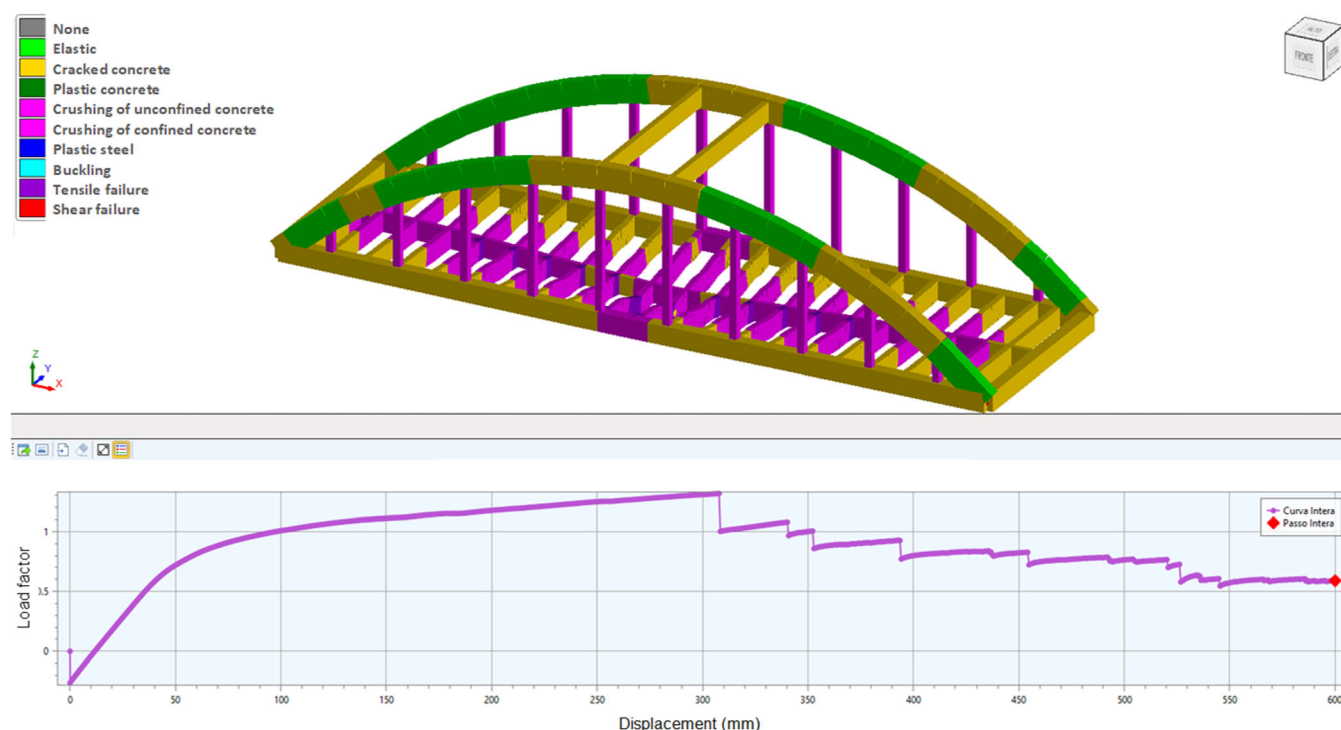


FIGURE 7 Damage state of the real configuration of the bridge.

From the analyses carried out considering the above assumptions, it is possible to identify the critical position of the load minimizing the robustness indicator.

Finally, on this configuration of loads in critical position, for all the hypothesized scenarios, an evaluation of the robustness index as a function of the time, that means by changing the  $x_{\text{corr}}$  corrosion depth from 0.50 to 3.00 mm ( $R = 3$ ), is done.

Operatively, after the creation of the bridge FEM model (Figure 6a), to define its ultimate bearing capacity and the related robustness index, reference is made to non-linear models with three embedded corrosion degradation models (Figure 6b–d), in which a non-linear static push-down analysis is performed under displacement control by modifying the control node with the position of the mobile load. This analysis procedure is carried out by the following steps:

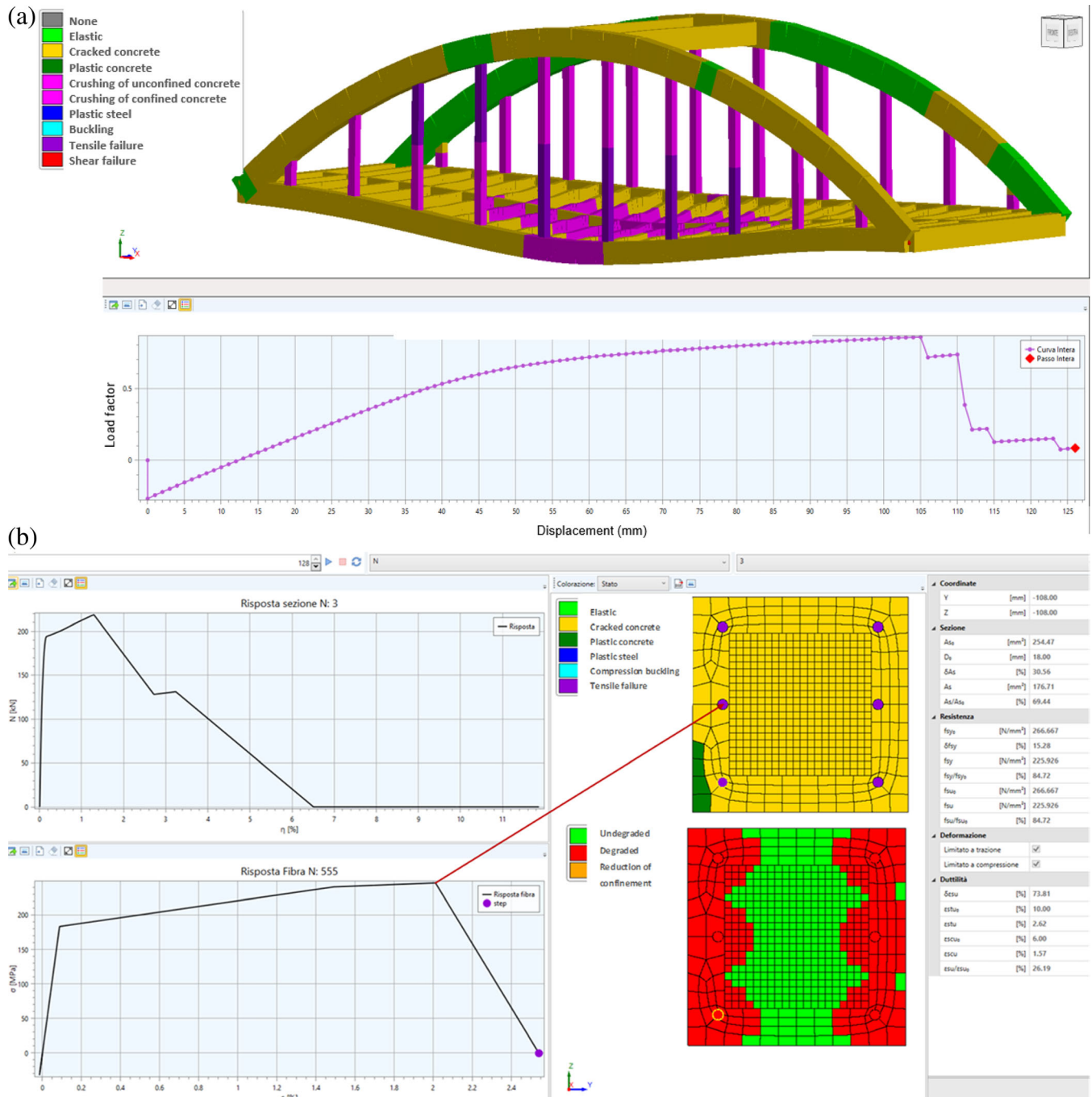


FIGURE 8 Damage state of the degraded configuration of the bridge (a) and details on both the failure of bars and the amount of deteriorated concrete portions of tie-beams (b).

- Apply to the FEM model with distributed plasticity the distributions of traffic loads for each combination of the scheme n.1;
- Perform non-linear static analyses to determine the multiplier of collapse loads according to the loading combination reported in Equation (8)<sup>11</sup>:

$$S_d = \gamma_G G_K + \lambda(\gamma_Q Q_{1K}) = R_d \left( f_{K\gamma/FC} \right) \quad (8)$$

- Calculate the minimum value of collapse load multipliers  $l_{MIN}$  as the distribution of loads from road traffic

changes. This identifies the robustness index  $I_R$  of the bridge;

- Verify the bridge robustness, which is acceptable if  $l_{MIN} = I_R \geq 1$ .

## 5 | ANALYSIS RESULTS

Results of the carried-out push-down analyses are expressed under form of both the damage state of structural elements and the overall behavior of the intact and damaged bridge under increasing loading. In particular,

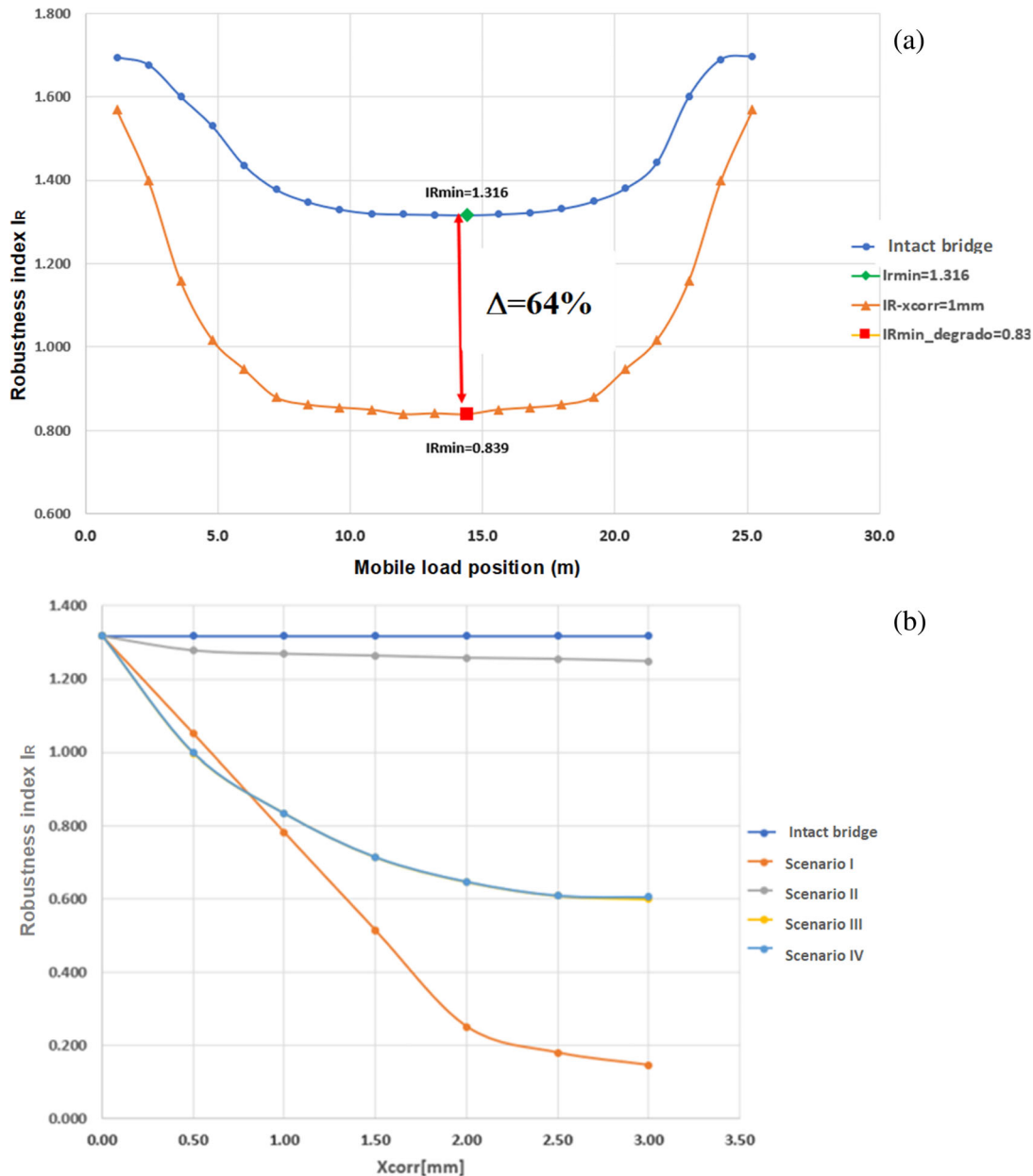


FIGURE 9 Variation of the robustness index versus (a) the position of the mobile loads and (b) the loading scenario and the corrosion depth ( $x_{corr} = 0.5/3.0$  mm).

the trend of the robustness index is reported as a function:

- of the degradation scenario, in order to identify, among the different loading positions considered, the critical one and the severity degree of the scenario in terms of robustness loss with respect to the intact bridge;
- of the time, that means with  $x_{\text{corr}}$  varying from 0.5 to 3.0 mm, under the degradation scenarios by considering the critical position of the mobile loads.

The damage state of the bridge in the actual configuration is plotted in Figure 7, where it is apparent that the tensile failure of reinforcement beams of both deck longitudinal beams and transverse beam is noticed. On the other hand, the damage state of tie-beams (scenario I) is characterized by the tensile failure of their reinforcement bars and the deck collapse, as shown in Figure 8a. Moreover, in Figure 8b the point of the curve when bars fail is shown and the degraded concrete parts are highlighted in the fiber model of the VSQNEXT calculation code, which is an applicative program of the FATANEXT NL software. In Figure 9a, the robustness index of both the original and degraded bridge is plotted as a function of the mobile loads position. The results show that the degraded bridge has an index about 64% than that of the original state bridge. In Figure 9b, the variation of the robustness index versus both the scenario variation and the considered corrosion level ( $x_{\text{corr}}$  from 0.5 to 3.0 mm) is plotted.

## 6 | CONCLUSIONS

The research activities performed on the inspected bridge have led toward the following conclusions:

- The minimum robustness index, which is strongly variable with the position of mobile loads, was determined considering the traffic load critical position, defined as a function of both the scenario and the extent of degradation (corrosion depth between 0.5 and 3.0 mm);
- The critical scenario was attained due to the tensile failure of corroded tie-beams, which induce the structural collapse with a reduction of the robustness index of about 50%–70%;
- The tie-beams played a fundamental role, since they gave to the bridge the right degree of redundancy, as well as the proper connection between the deck and the main arches to have a static scheme with eliminated thrust. When they prematurely collapsed, the arches and the deck were not able to redistribute the

stresses absorbed by the vertical elements, so that the sudden collapse of the bridge was attained.

## ACKNOWLEDGMENTS

The authors would like to acknowledge STACEC Srl company for the free supply of FATANEXT NL calculation code used for the analyses of the bridge herein presented.

## DATA AVAILABILITY STATEMENT

The data that support the findings of this study are available from the corresponding author upon reasonable request.

## ORCID

Antonio Formisano  <https://orcid.org/0000-0003-3592-4011>

## REFERENCES

1. Lo Bue F. Analysis and study of degradation effects induced by corrosion on rc structures (in Italian). Master thesis, University of Turin, Turin, Italy. 2018.
2. Rodriguez J, Ortega LM, Casal J. Load carrying capacity of concrete structures with corroded reinforcement. *Construct Build Mater*. 1997;11(4):239–48.
3. Val DV, Stewart MG, Melchers RE. Effect of reinforce corrosion on reliability of highway bridges. *Eng Struct*. 1998;20(11):1010–9.
4. Stewart MG. Mechanical behaviour of pitting corrosion of flexural and shear reinforcement and its effects on structural reliability of corroding RC beams. *Struct Saf*. 2009;31:19–30.
5. DuraCrete—Final technical report. Probabilistic performance based durability design of concrete structures, document BE95-1347/R17, European Brite-EuRam Programme, CUR, The Netherlands; 2000.
6. Du YG, Clark LA, Chan AHC. Effect of corrosion on ductility of reinforcing bars. *Mag Concr Res*. 2005;57(7):407–19.
7. Vergani M. Modelling of degradation of rc structures subjected to corrosion (in Italian). Master thesis, University of Milan, Milan, Italy. 2010.
8. Coronelli D, Gambarova P. Structural assessment of corroded reinforced concrete beams: modelling guidelines. *ASCE J Struct Eng*. 2004;130:1214–24.
9. Lo Giudice E, Di Marco GL, Gallo M, Mentione R. The bridge over the river Cassibile: a structure in r/c Bowstring scheme dating 1930. CTE Italian congress, October 27–28, Rome, Italy; 2016.
10. Santarella L, Miozzi E. In: Hoepli U, editor. Italian reinforced concrete bridges (in Italian). Milan, Italy: Ulrico Hoepli; 1948.
11. Ministry of Infrastructures and Transportations. Ministerial Decree 17/01/2018 “Upgrading of Technical Codes for Constructions” (in Italian). Official Gazette of the Italian Republic n. 42 emanated on 20/02/2018, Rome, Italy. 2018.
12. Felitti M, Oliveto F. In: Maggioli, editor. Evaluation of robustness into structural and geotechnical systems (in Italian). Santarcangelo di Romagna (RN), Italy: Maggioli; 2021.

## AUTHOR BIOGRAPHIES



Antonio Formisano  
Department of Structures for Engineering and Architecture  
University of Naples Federico II  
Naples, Italy



Matteo Felitti  
Engineering & Concrete Consulting  
Vietri di Potenza (PZ), Italy



Francesco Oliveto  
Freelance Engineer  
Viggianello (PZ), Italy



Lorenzo Mendicino  
Stacec srl  
Bovalino (RC), Italy

**How to cite this article:** Formisano A, Felitti M, Oliveto F, Mendicino L. The robustness of reinforced concrete tied arch bridges: A case study. *Structural Concrete*. 2023. <https://doi.org/10.1002/suco.202200374>